Geophysical Research Letters

RESEARCH LETTER
10.1029/2018GL077679

Key Points:
- We present the discovery of a significant influence of aerosol hygroscopicity on the magnitude of the aerosol first indirect effect (FIE) when aerosol optical quantities are used to estimate the FIE
- The one-unit enhancement in aerosol scattering coefficients due to the aerosol hygroscopicity leads to an underestimation of the magnitude of the FIE by about 23%
- This finding helps account for the systematic differences between observation-based and modeled-simulated FIE, especially for those derived from satellite-retrieved aerosol optical depth

Supporting Information:
- Figure S1
- Table S1

Correspondence to:
Z. Li,
zhanqing@umd.edu

Citation:
Liu, J., & Li, Z. (2018). Significant underestimation in the optically based estimation of the aerosol first indirect effect induced by the aerosol swelling effect. *Geophysical Research Letters*, *45*. https://doi.org/10.1029/2018GL077679

Received 28 FEB 2018
Accepted 23 APR 2018
Accepted article online 30 APR 2018

Significant Underestimation in the Optically Based Estimation of the Aerosol First Indirect Effect Induced by the Aerosol Swelling Effect

Jianjun Liu[1,2] and Zhanqing Li[1,3]

[1]Earth System Science Interdisciplinary Center and Department of Atmospheric and Oceanic Science, University of Maryland, College Park, MD, USA, [2]Laboratory of Environmental Model and Data Optima, Laurel, MD, USA, [3]State Key Laboratory of Earth Surface Process and Resource Ecology, College of Global Change and Earth System Science, Beijing Normal University, Beijing, China

Abstract Aerosol optical quantities have been widely employed as the proxy variables of cloud condensation nuclei concentration to study aerosol indirect effects (AIE). Due to the aerosol swelling effect, cloud condensation nuclei and aerosol optical quantities do not vary in harmony, leading to a bias in the estimation of the AIE. To identify and quantify this artifact, we employ extensive measurements of aerosol and cloud properties made at four sites in different continents that have distinct aerosol properties in terms of size and composition. One-unit enhancement in aerosol scattering coefficient by swelling effect is found to lead to a systematic underestimation of the first indirect effect (FIE) by about 23% that can result in an underestimation in the FIE-related radiative forcing by several W/m^2 depending on aerosol properties and relative humidity. This likely contributes significantly to the systematic difference between satellite-based estimates of the FIE and those simulated by general circulation models. Recommendations are made to make more sound comparisons of the AIE estimated from observations and model simulations.

Plain Language Summary Due to the limited measurements of cloud condensation nuclei concentration, the aerosol optical quantities such as aerosol optical depth have been widely employed to study the aerosol first indirect effect (FIE), which is one of the largest sources of uncertainties in climate studies. Aerosol optical quantities are significantly influenced by aerosol swelling effect, but cloud condensation nuclei are not, which can lead to a bias in the estimation of the FIE. Here we employed extensive measurements of aerosol and cloud properties made at four Atmospheric Radiation Measurement sites that have distinct aerosol types to identify and quantify this artifact. Our results reveal that one-unit enhancement in aerosol scattering coefficient due to aerosol swelling can result in underestimating the FIE by ~23%, which will lead the significant underestimation on the FIE-related radiative forcing. The finding helps account for the systematic differences between observation-based and modeled simulated FIE, especially for those derived from satellite-based measurements. It may also help explain some observed positive aerosol indirect effects values.

1. Introduction

Aerosol particles play significant roles in weather, climate, and various types of severe events through their direct and indirect effects (Li et al., 2016, 2017). The widely known Twomey effect (Twomey, 1977) is a key root cause for the widespread impact, which describes a decrease in cloud particle size with an increasing number of cloud particles for the same liquid water amount leading to a higher cloud albedo by more but smaller cloud droplets. This is often referred to as the aerosol first indirect effect (FIE), which has been estimated from satellite retrievals of cloud particle size and aerosol optical depth (AOD) or its derivative quantity called the aerosol index on regional (Liu et al., 2003; Menon et al., 2008; Nakajima et al., 2001; Yuan et al., 2008) and global (Bréon et al., 2002) scales. The aerosol FIE has also been studied at a few select sites using data from ground-based instruments (Feingold et al., 2003, 2006; Kim et al., 2003, 2008; Liu & Li, 2018; Liu et al., 2016; Ma et al., 2010; Pandithurai et al., 2009) and from aircraft in situ measurements (Flamant et al., 2018; Lu et al., 2008; Painemal & Zuidema, 2013).

These studies have reported that the magnitude of the FIE generally lies between 0.02 and 0.33, but anomalous values have also been reported (Panicker et al., 2010; Tang et al., 2014; Yuan et al., 2008). The FIE is subject to the influences of interactions and feedbacks with aerosol properties (e.g., aerosol vertical distribution, aerosol size distribution, and aerosol chemical properties) and cloud dynamical conditions (e.g., vertical velocity and vertical wind shear). Estimates of the FIE are also influenced by different analysis methods (Rosenfeld & Feingold, 2003), data spatial resolutions (McComiskey & Feingold, 2012), and meteorological conditions (Liu et al., 2016). A systematic discrepancy in the aerosol FIE was found based on coincident satellite and ground-based observations, which are sensitive to different parts of clouds (Liu et al., 2016). As such, the aerosol FIE has been regarded as one of the largest sources of uncertainties out of all climate forcing agents (IPCC, 2013; National Research Council, 2005; Tas et al., 2012).

The mechanism underlying the FIE is that aerosols can act as cloud condensation nuclei (CCN) and affect the number of cloud droplets and their droplet effective radius (DER). The FIE should thus be measured by the response of cloud properties to variations in CCN concentration. However, because of the high cost and complexity, in situ and ground-based observations of CCN concentration have been difficult to collect and few are on a global scale, especially over oceans despite a recent encouraging development of inferring CCN from satellite remote sensing (Rosenfeld et al., 2016). While the AOD has been commonly used as a proxy for CCN in FIE studies, the approximation suffers from serious uncertainties (Andreae, 2009; Liu & Li, 2014). The AOD represents the vertically integrated attenuation that depends not only on the number of particles but also on relative humidity (RH) and the size distribution, and is thus not a good proxy for the CCN even though it can be corrected to some extent (Liu & Li, 2014). A major uncertainty is incurred by aerosol hygroscopicity, which depends strongly on aerosol chemical composition (Jeong et al., 2007; Liu & Li, 2014). Aerosol hygroscopicity also conveys information about the enhancement of aerosol light scattering/extinction as RH increases. Meanwhile, the aerosol absorption may be augmented by the humidification effect for light-absorbing aerosols with a hygroscopic coating (Peng et al., 2016; Wang et al., 2013), which could potentially be an additional uncertainty source for using AOD as a proxy for CCN. Studies on the relationship between cloud cover and AOD show that the aerosol humidification effect can explain about a quarter of the observational correlation between cloud cover and AOD (Jeong & Li, 2010) and is the dominant contributor to the modeled cloud cover-AOD relationship (Quaas et al., 2009, 2010).

However, few studies have examined the extent of the contribution of the enhancement in aerosol optical properties due to aerosol swelling to the FIE, which is possibly one of the main reasons behind the large uncertainties in aerosol-cloud interaction (ACI) studies using satellite retrievals. Feingold and McComiskey (2016) and Seinfeld et al. (2016) have pointed out that the contributions of aerosol hygroscopicity and composition to the FIE are still ambiguous and that further observationally based evaluations are still needed.

The objective of this study is to examine the adverse influence of aerosol hygroscopicity on the FIE and to estimate the contribution of this artifact to the magnitude of the FIE derived from measurements made by a large suite of instruments at fixed and mobile Atmospheric Radiation Measurement (ARM) Climate Research Facility (ACRF) sites located in regions around the world with different meteorological conditions and diverse aerosol types with distinct aerosol compositions and sizes. The findings have significant implications for both ACI studies based on satellite and ground-based aerosol optical quantities and for explaining discrepancies between observation-based estimates of the FIE and model simulations of the FIE.

2. Data and Methods

2.1. Experimental Sites

Data from four ACRF sites, representing different climate conditions and aerosol types, were selected. The fixed sites are located in the U.S. Southern Great Plains (SGP) and on Graciosa Island in the Azores (GRW). The mobile facility sites are located in the Ganges Valley in India (PGH) and at ShouXian (SX) in China. Detailed information about each site is listed in Table S1 in the supporting information and can also be found at http://www.arm.gov/sites.

10.1029/2018GL077679

2.2. Aerosol Scattering Coefficients and Hygroscopicity

Total aerosol scattering coefficients (σ) of aerosol particles with diameters less than 1 μm and 10 μm were measured by two 3-wavelength (450, 550, and 700 nm) TSI Model 3653 nephelometers. The σ associated with aerosol particles with diameters less than 10 μm were used in this study. One instrument measured σ under dry conditions (RH = ~40%) and the other instrument measured σ under varying RH conditions (~40% to ~90%). The aerosol hygroscopic growth factor is defined as the ratio of σ at a given RH to that at a low reference RH (RH_{Ref}):

$$f_{\sigma,\mathrm{RH}} = \frac{\sigma_{(\mathrm{RH})}}{\sigma_{(\mathrm{RH_{Ref}})}}. \tag{1}$$

The hygroscopic growth factor at RH = 85% and RH_{Ref} = 40% is then written as $f_{\mathrm{RH}(85\%/40\%)}$, which is denoted as f_{RH} in this study. A two-parameter function has been widely used to describe the RH dependence of σ:

$$f_{\sigma,\mathrm{RH}} = a \times \left(1 - \frac{\mathrm{RH}(\%)}{100}\right)^{-b}, \tag{2}$$

where *a* and *b* are determined by fitting σ measured at varying RH levels (Jefferson, 2011). By fitting the function with observational data from the study sites, the parameters *a* and *b* can be derived, from which σ can be estimated at any ambient RH level:

$$\sigma(\mathrm{amb}) = \sigma(\mathrm{dry}) \frac{\left(1 - \frac{\mathrm{RH_{amb}}}{100}\right)^{-b}}{\left(1 - \frac{\mathrm{RH_{dry}}}{100}\right)^{-b}}. \tag{3}$$

2.3. Cloud Optical and Microphysical Properties

The cloud optical depth (COD) retrieved in this study is based on ground measurements of downwelling zenith radiance measured by a two-channel (673 and 870 nm) narrow field-of-view radiometer with a 5.7° field of view (Chiu et al., 2006; Liu et al., 2013; Marshak et al., 2004). Narrow field-of-view radiance measurements are quantified and corrected by comparing them with Aerosol Robotic Network Sun photometer radiance measurements, which are considered to be accurate (Holben et al., 1998) at the four sites as shown by Chiu et al. (2006; Figure S1). The COD retrieved by this method has been validated through comparisons with retrievals from other surface-based and satellite-based methods (Chiu et al., 2006; Liu et al., 2013; Marshak et al., 2004).

The cloud liquid water path (LWP) was retrieved using the statistical approach proposed by Liljegren et al. (2001) and Liljegren and Lesht (2004) applied to atmospheric brightness temperature measurements made by a microwave radiometer or a microwave radiometer profiler. Typical uncertainties in LWP retrievals from microwave radiometers are ~20 g/m^2 for LWP $<$ 200 g/m^2 and ~10% for LWP $>$ 200 g/m^2 (Liljegren et al., 2001). DER is calculated from temporally matched retrievals of COD and LWP using the following equation:

$$\mathrm{COD} = \frac{3\mathrm{LWP}}{2\rho_w \mathrm{DER}}, \tag{4}$$

where ρ_w is the density of water. Micropulse lidar measurements were used to determine cloud base heights at the SGP, GRW, and SX sites using the methodology developed by Wang and Sassen (2001). Ceilometer measurements were used to determine cloud base heights at the PGH site.

In this study, data corresponding to LWP $<$ 50 g/m^2 and LWP $>$ 700 g/m^2 were excluded to avoid very thin or broken cloud cover, postprecipitation conditions (McComiskey et al., 2009), and potential precipitation contamination (Dong et al., 2008). Clouds with bases higher than 1.0 km and with DER $>$ 25 μm were also excluded because these values are unrealistic for low-level clouds (Bulgin et al., 2008).

3. Results

Statistics summarizing cloud microphysical and aerosol properties at each site are listed in Table S2. The largest mean LWPs occur at the PGH site (192 ± 141 g/m^2) and at the SX site (171 ± 119 g/m^2). Mean LWP at the SGP and GRW sites are roughly the same. Mean COD is the largest at the PGH site (38.4 ± 21.5), followed by mean COD at the SX (37.3 ± 24.9), SGP (35.9 ± 18.2), and GRW (31.8 ± 17.6) sites. The largest and smallest mean DER is found at the PGH and SGP sites (8.3 ± 4.9 μm and 7.0 ± 3.3 μm, respectively). The largest f_{RH} is found at the GRW site. This is because sea salt aerosols with strong hygroscopicities dominate over this

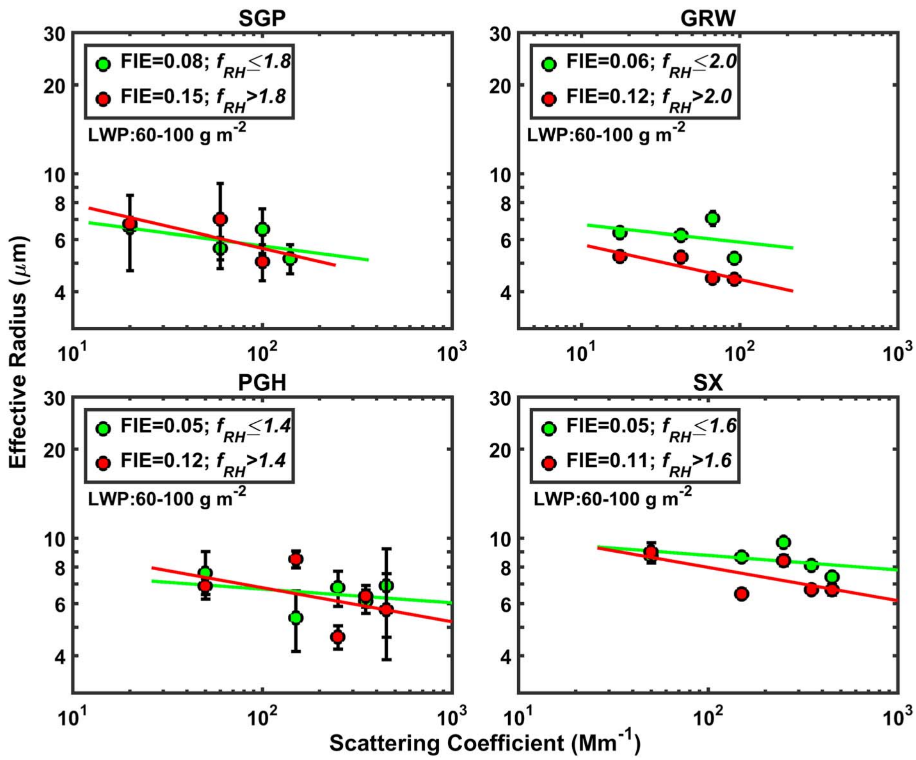

Figure 1. Cloud effective radius as a function of dry aerosol scattering coefficient at 450 nm at the SGP, GRW, PGH, and SX sites for samples with f_{RH} less than and greater than the site-specific threshold value. LWP is constrained to the range of 60–100 g/m^2. Green dots represent data corresponding to f_{RH} less than the site-specific threshold value, and red dots represent data corresponding to f_{RH} greater than the site-specific threshold value. Green and red lines represent the best fit lines through each group of data. FIE stands for the aerosol first indirect effect. LWP = liquid water path.

area. The smallest value of f_{RH} is found at the PGH site, which suggests that aerosols with relatively low hygroscopicity are prevalent over this region. The noticeably different f_{RH} seen at each site suggests that aerosols with different compositions dominate at each site. Very high aerosol loading is seen at the SX site (mean σ = 451 ± 477 M/m). Aerosol loading is lowest at the GRW site (mean σ = 34 ± 23 M/m). These results show that much greater differences in aerosol composition and aerosol loading exist from site to site.

The aerosol FIE was estimated using the linear regression slope of relationship between DER and σ in log-log scale at constant LWP. Figure 1 shows DER as a function of dry σ in two f_{RH} bins at each site. LWP is constrained to the range of 60–100 g/m^2. Threshold values of f_{RH} used to define the two bins are the median values of f_{RH} for data with LWP ranging from 60–100 g/m^2. Accompanying statistics listing the mean and standard deviation of σ, DER, and COD in each f_{RH} bin at each site are given in Table S3. At the SGP and PGH sites, larger values of mean σ are found for aerosol samples with low f_{RH}, but at the GRW and SX sites, larger values of mean σ are found for aerosol samples with high f_{RH}. At each site, the f_{RH} bin with the largest σ also has the largest COD and the smallest DER. These results are consistent with the results reported by Kim et al. (2003) who showed that COD is enhanced by increased aerosol loading.

The magnitude of the FIE for aerosol particles with relatively large f_{RH} is greater than the magnitude of the FIE for aerosol particles with relatively smaller f_{RH} at each site (legends in Figure 1). This suggests that aerosol particles with higher hygroscopicities have a greater effect on DER. Aerosol particles with higher hygroscopicities are generally more readily activated into CCN. This means that ACIs are more sensitive to aerosols, resulting in a relatively stronger FIE. Model simulations have shown a weak relationship between DER and AOD and at times, a positive correlation between DER and AOD due to a decrease in activated aerosols when aerosols contain increasing amounts of slightly soluble organics (Yuan et al., 2008). Aerosol composition appears to play a role in determining the ultimate magnitude of the Twomey effect (McComiskey et al., 2009). The DER is nonlinear with respect to aerosol concentration, showing the highest sensitivity in the transition from clean to slightly polluted conditions (Koren et al., 2014). The similar ranges of aerosol loading for

10.1029/2018GL077679

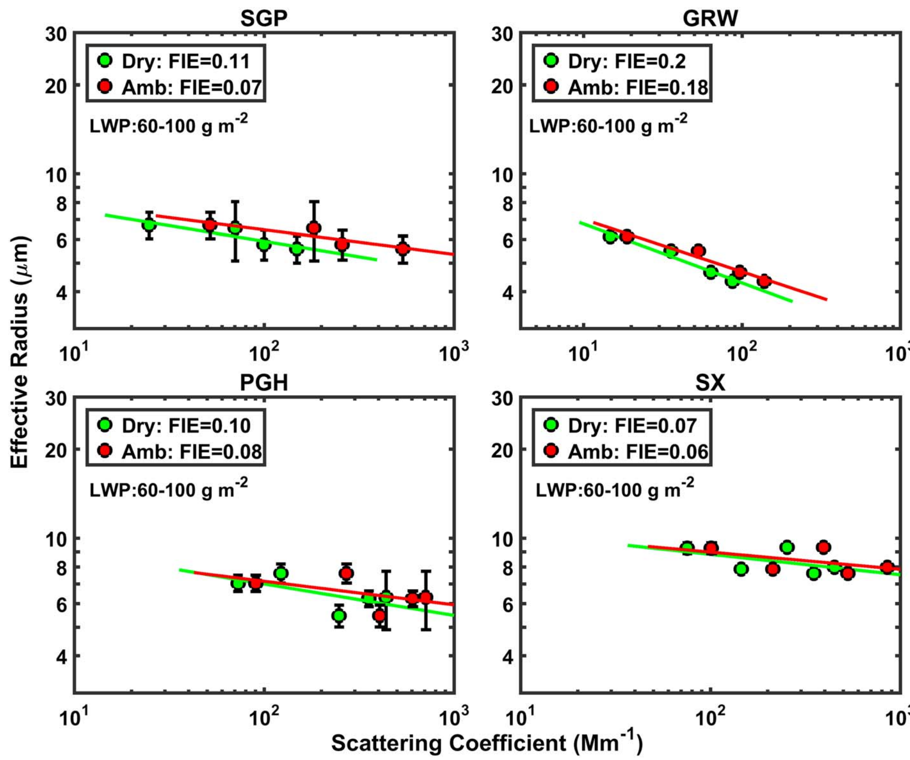

Figure 2. Cloud effective radius as a function of dry aerosol scattering coefficient at 450 nm (green dots) and ambient aerosol scattering coefficient at 450 nm (red dots) at each site (SGP, GRW, PGH, and SX). LWP is constrained to the range of 60–100 g/m^2. FIE stands for the aerosol first indirect effect. LWP = liquid water path.

smaller and larger f_{RH} cases at each site (Figure 1 and Table S3) suggest that the aerosol loading condition is not the main reason behind the differences in the FIE for the smaller and larger f_{RH} samples.

The AOD and aerosol extinction coefficients measured under ambient conditions depend not only on the aerosol loading but also on particle size and atmospheric humidity due to aerosol swelling. Liu and Li (2014) have shown that RH significantly influences the CCN estimation from AOD retrievals and aerosol extinction/scattering coefficient measurements. Figure 2 shows DER as a function of σ under dry and ambient RH conditions for the LWP range of 60–100 g/m^2 at each site. Mean values of σ under dry and ambient conditions, respectively, are 60.3 ± 39.4 M/m and 160.3 ± 140.8 M/m at the SGP site, 32.5 ± 22.2 M/m and 47.4 ± 38.4 M/m at the GRW site, 214.2 ± 129.3 M/m and 350.8 ± 190.5 M/m at the PGH site, and 306.2 ± 125.7 M/m and 471.9 ± 228.0 M/m at the SX site. The enhancements in σ due to the aerosol swelling effect (Δσ), defined as the ratio of the difference in σ under ambient RH conditions and dry RH conditions to σ under dry RH conditions, are large with magnitudes of 165.8%, 45.8%, 63.8%, and 54.1% at the SGP, GRW, PGH, and SX sites, respectively. The FIE estimated using the dry σ is larger than that using the ambient σ at all four sites, and especially at sites where the largest enhancement in σ due to the swelling effect is found. This is mainly because DER is nonlinear with respect to aerosol concentration, showing a higher sensitivity in the transition from clean to slightly polluted conditions than from clean to highly polluted conditions (Koren et al., 2014). It is also the reason that for the same amount of scattering, there are more aerosol particles under dry conditions than under wet conditions. So per unit change of aerosol scattering, there are more changes in CCN concentration.

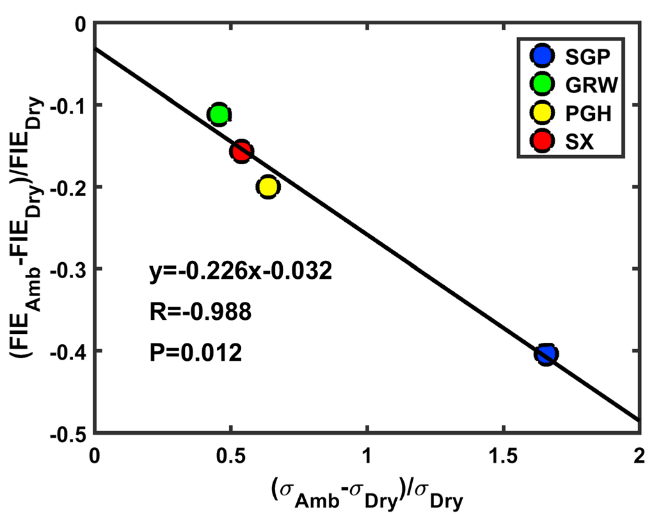

Figure 3. Changes in FIE [(FIE$_{Amb}$ − FIE$_{Dry}$)/FIE$_{Dry}$] estimated by using the ambient σ and the dry σ as a function of the enhancement in σ [(σ$_{Amb}$ − σ$_{Dry}$)/σ$_{Dry}$] due to aerosol swelling effects from dry to ambient relative humidity conditions at each site.

The differences in the FIE for the two cases in Figure 3 at all sites are attributed to the ambient and dry aerosol scattering coefficients that are used in calculating the FIE since all other potential factors (e.g., cloud samples and meteorological variables) are kept the same in the two cases. The contribution of aerosol humidification to the FIE, expressed as the change in FIE (dFIE), is estimated using the ambient σ and the dry σ [i.e., dFIE = $(FIE_{amb} - FIE_{dry})/FIE_{dry}$]. The dFIE as a function of dσ ($(\sigma_{Amb} - \sigma_{Dry})/\sigma_{Dry}$) is shown in Figure 3. The increase in σ induced by aerosol swelling enhanced the magnitude of the decrease in the FIE. When σ increases by one unit, the calculated magnitude of the FIE can decrease by ~23%. Twomey (1974) reported a typical FIE value of ~0.27. Our result implies that when aerosol optical properties such as AOD and/or extinction are used as CCN proxies to estimate the FIE, the one-unit enhancement of aerosol optical properties due to the aerosol swelling effect will result in an underestimation of 0.06 for the FIE. By using Santa Barbara DISORT Atmospheric Radiative Transfer model simulations, McComiskey and Feingold (2008) found that an uncertainty of 0.05 in the FIE could result in a local radiative forcing error of −3 to −10 W/m^2 depending on the properties of the aerosols.

Previous studies have indicated that atmospheric humidity and large-scale dynamic and thermodynamic conditions influence ACIs (Feingold et al., 2003; Gryspeerdt et al., 2014; Liu et al., 2016; Liu & Li, 2018; Su et al., 2010; Yuan et al., 2008). The vertical velocity at 700 hPa (ω) and lower tropospheric stability (LTS) have been used to constrain the dynamic and thermodynamic conditions (Bony et al., 2004; Lebsock et al., 2008; Matsui et al., 2004; Su et al., 2010). They are thus also examined in this study. The LTS is calculated as the difference between the potential temperature of the free troposphere (700 hPa) and the potential temperature at the surface. Both quantities are obtained from the European Centre for Medium-Range Weather Forecasts (ECMWF) model runs for ARM analysis with an hourly resolution for a 0.56° × 0.56° box centered on the site (European Centre for Medium-Range Weather Forecasts (ECMWF), 1994). While the reanalysis is not as accurate as actual sounding data, the latter are too few for this investigation. Figures S2a–S2c show the mean values and standard deviations of surface RH, ω, and LTS for aerosol particle samples with low and high f_{RH} at each site. Under both low- and high-f_{RH} conditions, RH, ω, and LTS are similar at all sites. This suggests that meteorological conditions are not the main reason behind the difference in the estimated FIE for cases with low and high f_{RH}. Figures S2d–S2f show the mean values and standard deviations of surface RH, ω, and LTS under low and high aerosol loading conditions for aerosol samples with lower and higher f_{RH} at each site. Samples under low and high aerosol loading conditions in the f_{RH} bins are defined as those with σ smaller and larger than the lower and upper one quarter of the total instantaneous σ in that f_{RH} bin, respectively. There is no significant difference in any of the meteorological variables between low and high aerosol loading conditions for the smaller and larger f_{RH} cases at all sites, suggesting that the decrease in DER with increasing σ is not explained by variations in meteorological variables from low to high aerosol loading conditions.

4. Implication of the Finding

Before interpreting the above results, one must first bear in mind the limitations of the approach due to numerous assumptions made which include, among others, (1) AOD measured in the clear column is proportional (not necessarily identical) to the aerosol extinction near cloud base, (2) CCN at cloud base is proportional to aerosol extinction, and (3) CCN is proportional to cloud droplet number concentration. It is beyond the scope of this study to assess the effectiveness of the approach itself. The intent of the study is to demonstrate an often overlooked factor that can undermine the validity of using the correlations between aerosol measurements made in the clear-sky column and cloud microphysics in nearby cloud cells.

The above findings imply that the FIE is underestimated when AOD or aerosol scattering/extinction coefficients at ambient RH conditions are used as a proxy for CCN to study ACIs. This is especially relevant to aerosol indirect effect studies based on satellite retrievals that commonly use AOD and/or aerosol extinction coefficients without considering the aerosol swelling effect. This is especially so in humid regions and in near-cloud regions where AODs and extinction coefficients are significantly enhanced due in part to aerosol humidification and the consequential growth of aerosol particles in the moist cloud environment (Jeong & Li, 2010; Marshak et al., 2008; Yang et al., 2014).

The finding is consistent with that of Yuan et al. (2008) who found a highly variable FIE that is most sensitive to the atmospheric moisture content by analyzing Moderate Resolution Imaging Spectroradiometer-retrieved AOD and cloud particle size with meteorological quantities from the ECMWF reanalysis. The slope of their DER-AOD relationship is negative with a larger magnitude in the dry interior region of the continental United States, which decreases as moisture increases and even becomes positive in the very humid region of the Gulf coast (Yuan et al., 2008). This is mainly because an increase in water vapor is accompanied by an increase in drop collision-coalescence events and a reduction in cloud drop number concentration for the same AOD, resulting in a decrease in the effect of aerosols on DER (McComiskey et al., 2009). While the finding of this study helps explain the dependence of the FIE on moisture, we cannot attribute it entirely to this effect which would require simultaneous measurements made across the same region as covered by the satellite. We can, however, make a recommendation for any field campaign to make either CCN (best) or aerosol scattering measurements at the same humidity in determining the FIE for the sake of cross comparison. If only AOD or other optical quantities are available at ambient conditions, a correction should be made to get a better proxy for CCN (Liu & Li, 2014).

Previous studies have shown systematic discrepancies in ACIs between general circulation model (GCM) simulations and observations. GCM simulations tend to overestimate the cooling of ACIs and are more susceptible to aerosols compared with observations (e.g., Chen et al., 2016; Quaas et al., 2009; Quaas & Boucher, 2005; Quaas et al., 2004). Multiple mechanisms have been proposed to identify the possible factors contributing to the observation-model discrepancy, such as the dispersion effect whereby changes in aerosol properties alter the spectral shape of the cloud droplet size distribution in addition to droplet number concentrations (e.g., Chen et al., 2016; Liu & Daum, 2002; Pandithurai et al., 2012), the turbulent entrainment-mixing process (e.g., Grabowski, 2006; Kim et al., 2003), the autoconversion process (e.g., Michibata et al., 2016), and the buffering effect (Stevens & Feingold, 2009). The obvious discrepancies in the cloud cover-AOD and LWP-AOD relationship obtained from GCM simulations and from observations have been partly attributed to the aerosol swelling in regions where humidity is high and clouds are coincidentally present (Grandey et al., 2013; Neubauer et al., 2017; Quaas et al., 2010). The finding from our study that optically based methods may underestimate the FIE due to the aerosol swelling effect provides another possible explanation for the discrepancy between measurements and GCM estimations. As such, we would recommend to use CCN or any proxy variable made under dry or fixed humidity in computing the AIE for the sake of cross comparison between observation and modeling, or among different observations.

5. Summary

The effects of aerosols on cloud microphysical properties remain one of the largest uncertainties among all climate forcing agents/mechanisms. They have been shown to be sensitive to meteorological conditions (e.g., vertical velocity), the scale and resolution of observations, as well as aerosol concentration, size, and chemistry. In this study, the influence of aerosol hygroscopicity (f_{RH}), which strongly depends on aerosol composition, on the relationship between aerosols and DER, is examined based on measurements of aerosol and cloud properties made at four ACRF sites located around the world. Overall, the magnitude of the FIE for aerosol particles with stronger f_{RH} is larger than that for aerosol particles with weaker f_{RH}, suggesting that aerosols with higher hygroscopicities have a seemingly greater effect on cloud microphysical properties. Aerosol particles with higher hygroscopicities are generally more readily activated into CCN and the resulting cloud droplets more readily grow as well, and thus in a relatively stronger FIE. This suggests that aerosol composition also plays an important role in ACIs.

Aerosol scattering coefficients are enhanced due to the aerosol swelling effect. Magnitudes of the FIE estimated using dry aerosol scattering coefficients were greater than those based on ambient aerosol scattering coefficients at all four sites. When aerosol scattering coefficients were enhanced by one unit due to aerosol swelling, the magnitude of the FIE decreased by up to ~23%, which may contribute to a positive FIE as noted in some previous observation-based studies. This corresponds to an underestimation of the FIE-induced radiative forcing of -3 to -10 W/m^2 when AOD or aerosol scattering/extinction coefficients under ambient RH conditions are used as a proxy for CCN. By contrast, model-based estimations of the FIE usually do not account for the hygroscopic effect, leading to potentially artificial discrepancies which ought to be accounted for in observation-model intercomparison studies of the FIE. For the sake of comparing AIE between observation and modeling or among observations, it is recommended to use (in the order of preference) CCN (best), aerosol number concentration, dry mass, scattering coefficient measured under dry or constant RH, ambient AOD (worst) for the sake of comparison. Whenever feasible, a correction should be made for the swelling effect.

Acknowledgments
Ground-based observations from the U.S. Southern Great Plains, Graciosa Island in the Azores, the Ganges Valley in India, and ShouXian, China, were obtained from the Department of Energy Atmospheric Radiation Measurement (ARM) Program (Data can be accessed at http://www.archive.arm.gov/discovery/). The large-scale dynamic and thermodynamic data were obtained from the European Centre for Medium-Range Weather Forecasts (ECMWF) model runs for ARM analysis provided by the ECMWF. M. Cribb helped edit the manuscript. The study is supported by the following research grants: the National Science Foundation of US (AGS1534670) and China (91544217) and the Key R&D Program (2017YFC1501702).

References

Andreae, M. O. (2009). Correlation between cloud condensation nuclei concentration and aerosol optical thickness in remote and polluted regions. *Atmospheric Chemistry and Physics*, *9*(2), 543–556. https://doi.org/10.5194/acp-9-543-2009

Bony, S., Dufresne, J. L., Le Treut, H., Morcrette, J. J., & Senior, C. (2004). On dynamic and thermodynamic components of cloud changes. *Climate Dynamics*, *22*(2-3), 71–86. https://doi.org/10.1007/s00382-003-0369-6

Bréon, F. M., Tanré, D., & Generosol, S. (2002). Aerosol effect on cloud droplet size monitored from satellite. *Science*, *295*(5556), 834–838. https://doi.org/10.1126/science.1066434

Bulgin, C. E., Palmer, P. I., Thomas, G. E., Arnold, C. P. G., Campmany, E., Carboni, E., et al. (2008). Regional and seasonal variations of the Twomey indirect effect as observed by the ATSR-2 satellite instrument. *Geophysical Research Letters*, *35*, L02811. https://doi.org/10.1029/2007GL031394

Chen, J., Liu, Y., Zhang, M., & Peng, Y. (2016). New understanding and quantification of the regime dependence of aerosol-cloud interaction for studying aerosol indirect effects. *Geophysical Research Letters*, *43*(4), 1780–1787. https://doi.org/10.1002/2016GL067683

Chiu, J. C., Marshak, A., Knyazikhin, Y., Wiscombe, W. J., Barker, H. W., Barnard, J. C., & Luo, Y. (2006). Remote sensing of cloud properties using ground-based measurements of zenith radiance. *Journal of Geophysical Research*, *111*, D16201. https://doi.org/10.1029/2005JD006843

Dong, X., Minnis, P., Xi, B., Sun-Mack, S., & Chen, Y. (2008). Comparison of CERES-MODIS stratus cloud properties with ground-based measurements at the DOE ARM Southern Great Plains site. *Journal of Geophysical Research*, *113*, D03204. https://doi.org/10.1029/2007JD008438

European Centre for Medium-Range Weather Forecasts (ECMWF) (1994). The description of the ECMWF/WCRP Level III—A global atmospheric data archive. Retrieved from http://cedadocs.ceda.ac.uk/1109/

Feingold, G., Eberhard, W. L., Veron, D. E., & Previdi, M. (2003). First measurements of the Twomey indirect effect using ground-based remote sensors. *Geophysical Research Letters*, *30*(6), 1287. https://doi.org/10.1029/2002GL016633

Feingold, G., Furrer, R., Pilewskie, P., Remer, L. A., Min, Q., & Jonsson, H. (2006). Aerosol indirect effect studies at Southern Great Plains during the May 2003 intensive operations period. *Journal of Geophysical Research*, *111*, D05S14. https://doi.org/10.1029/2004JD005648

Feingold, G., & McComiskey, A. (2016). ARM's aerosol-cloud-precipitation research (aerosol indirect effects). *Meteorological Monographs*, *57*, 22.1–22.15. https://doi.org/10.1175/AMSMONOGRAPHS-D-15-0022.1

Flamant, C., Knippertz, P., Fink, A. H., Akpo, A., Brooks, B., Chiu, C. J., et al. (2018). The dynamics-aerosol-chemistry-cloud interactions in West Africa field campaign: Overview and research highlights. *Bulletin of the American Meteorological Society*, *99*(1), 83–104. https://doi.org/10.1175/BAMS-D-16-0256.1

Grabowski, W. W. (2006). Indirect impact of atmospheric aerosols in idealized simulations of convective-radiative quasi equilibrium. *Journal of Climate*, *19*(18), 4664–4682. https://doi.org/10.1175/JCLI3857.1

Grandey, B. S., Stier, P., & Wagner, T. M. (2013). Investigating relationships between aerosol optical depth and cloud fraction using satellite, aerosol reanalysis and general circulation model data. *Atmospheric Chemistry and Physics*, *13*(6), 3177–3184. https://doi.org/10.5194/acp-13-3177-2013

Gryspeerdt, E., Stier, P., & Partridge, D. G. (2014). Satellite observations of cloud regime development: The role of aerosol processes. *Atmospheric Chemistry and Physics*, *14*(3), 1141–1158. https://doi.org/10.5194/acp-14-1141-2014

Holben, B. N., Eck, T. F., Slutsker, I., Tanré, D., Buis, J. P., Setzer, A., et al. (1998). AERONET—A federated instrument network and data archive for aerosol characterization. *Remote Sensing of Environment*, *66*(1), 1–16. https://doi.org/10.1016/S0034-4257(98)00031-5

IPCC (2013). Climate Change 2013: The Physical Science Basis. Contribution of Working Group I to the Fifth Assessment Report of the Intergovernmental Panel on Climate Change. In T. F. Stocker, et al. (Eds.), (1535 pp). Cambridge, UK and New York: Cambridge University Press. https://doi.org/10.1017/CBO9781107415324

Jefferson, A. (2011). *Aerosol observing system (AOS) handbook* (Rep. ARM-TR-014, U.S). Washington, DC: Department of Energy.

Jeong, M. J., & Li, Z. (2010). Separating real and apparent effects of cloud, humidity, and dynamics on aerosol optical thickness near cloud edges. *Journal of Geophysical Research*, *115*, D00K32. https://doi.org/10.1029/2009JD013547

Jeong, M. J., Li, Z., Andrews, E., & Tsay, S.-C. (2007). Effect of aerosol humidification on the column aerosol optical thickness over the Atmospheric Radiation Measurement Southern Great Plains site. *Journal of Geophysical Research*, *112*, D10202. https://doi.org/10.1029/2006JD007176

Kim, B. G., Miller, M. A., Schwartz, S. E., Liu, Y., & Min, Q. (2008). The role of adiabaticity in the aerosol first indirect effect. *Journal of Geophysical Research*, *113*, D05210. https://doi.org/10.1029/2007JD008961

Kim, B. G., Schwartz, S. E., Miller, M. A., & Min, Q. (2003). Effective radius of cloud droplets by ground-based remote sensing: Relationship to aerosol. *Journal of Geophysical Research*, *108*(D23), 4740. https://doi.org/10.1029/2003JD003721

Koren, I., Dagan, G., & Altaratz, O. (2014). From aerosol-limited to invigoration of warm convective clouds. *Science*, *344*(6188), 1143–1146. https://doi.org/10.1126/science.1252595

Lebsock, M. D., Stephens, G. L., & Kummerow, C. (2008). Multi-sensor satellite observations of aerosol effects on warm clouds. *Journal of Geophysical Research*, *113*, D15205. https://doi.org/10.1029/2008JD009876

Li, Z., Lau, W. K.-M., Ramanathan, V., Wu, G., Ding, Y., Manoj, M. G., et al. (2016). Aerosol and monsoon climate interactions over Asia. *Reviews of Geophysics*, *54*, 866–929. https://doi.org/10.1002/2015RG000500

Li, Z., Rosenfeld, D., & Fan, J. (2017). Aerosols and their impact on radiation, clouds, precipitation and severe weather events. *Oxford Research Encyclopedia of Environmental Science*. https://doi.org/10.1093/acrefore/9780199389414.013.126

Liljegren, J. C., Clothiaux, E. E., Mace, G. G., Kato, S., & Dong, X. (2001). A new retrieval for cloud liquid water path using a ground-based microwave radiometer and measurements of cloud temperature. *Journal of Geophysical Research*, *106*, 14,485–14,500. https://doi.org/10.1029/2000JD900817

Liljegren, J. C., & Lesht, B. M. (2004). Preliminary results with the twelve channel microwave radiometer profiler at the North Slope of Alaska Climate Research Facility. In *Fourteenth ARM Science Team Meeting Proceedings*. Albuquerque, New Mexico.

Liu, G., Shao, H., Coakley, J. A. Jr., Curry, J. A., Haggerty, J. A., & Tschudi, M. A. (2003). Retrieval of cloud droplet size from visible and microwave radiometric measurements during INDOEX: Implication to aerosols' indirect radioactive effect. *Journal of Geophysical Research*, *108*(D1), 4006. https://doi.org/10.1029/2001JD001395

Liu, J., & Li, Z. (2014). Estimation of cloud condensation nuclei concentration from aerosol optical quantities: Influential factors and uncertainties. *Atmospheric Chemistry and Physics*, *14*(1), 471–483. https://doi.org/10.5194/acp-14-471-2014

Liu, J., & Li, Z. (2018). First surface-based estimation of the aerosol indirect effect over a site in southeastern China. *Advances in Atmospheric Sciences*, *35*(2), 169–181. https://doi.org/10.1007/s00376-017-7106-2

Liu, J., Li, Z., & Cribb, M. (2016). Response of marine boundary layer cloud properties to aerosol perturbations associated with meteorological conditions from the 19-month AMF-Azores campaign. *Journal of the Atmospheric Sciences*, *73*(11), 4253–4268. https://doi.org/10.1175/JAS-D-15-0364.1

Liu, J., Li, Z., Zheng, Y., Chiu, J. C., Zhao, F., Cadeddu, M., et al. (2013). Cloud optical and microphysical properties derived from ground-based and satellite sensors over a site in the Yangtze Delta region. *Journal of Geophysical Research: Atmospheres*, *118*, 9141–9152. https://doi.org/10.1002/jgrd.50648

Liu, Y., & Daum, P. H. (2002). Anthropogenic aerosols: Indirect warming effect from dispersion forcing. *Nature*, *419*(6907), 580–581. https://doi.org/10.1038/419580a

Lu, M. L., Feingold, G., Jonsson, H. H., Chuang, P. Y., Gates, H., Flagan, R. C., & Seinfeld, J. H. (2008). Aerosol-cloud relationships in continental shallow cumulus. *Journal of Geophysical Research*, *113*, D15201. https://doi.org/10.1029/2007JD009354

Ma, J., Chen, Y., Wang, W., Yan, P., Liu, H., Yang, S., et al. (2010). Strong air pollution causes widespread haze clouds over China. *Journal of Geophysical Research*, *115*, D18204. https://doi.org/10.1029/2009JD013065

Marshak, A., Knyazikhin, Y., Evans, K. D., & Wiscombe, W. J. (2004). The "RED versus NIR" plane to retrieve broken-cloud optical depth from ground-based measurements. *Journal of the Atmospheric Sciences*, *61*(15), 1911–1925. https://doi.org/10.1175/1520-0469(2004)061%3C1911:TRVNPT%3E2.0.CO;2

Marshak, A., Wen, G., Coakley, J. A. Jr., Remer, L. A., Loeb, N. G., & Cahalan, R. F. (2008). A simple model for the cloud adjacency effect and the apparent bluing of aerosols near clouds. *Journal of Geophysical Research*, *113*, D14S17. https://doi.org/10.1029/2007JD009196

Matsui, T., Masunaga, H., Pielke, R. A. S., & Tao, W. K. (2004). Impact of aerosols and atmospheric thermodynamics on cloud properties within the climate system. *Geophysical Research Letters*, *31*, L06109. https://doi.org/10.1029/2003GL019287

McComiskey, A., & Feingold, G. (2008). Quantifying error in the radiative forcing of the first aerosol indirect effect. *Geophysical Research Letters*, *35*, L02810. https://doi.org/10.1029/2007GL032667

McComiskey, A., & Feingold, G. (2012). The scale problem in quantifying aerosol indirect effects. *Atmospheric Chemistry and Physics*, *12*(2), 1031–1049. https://doi.org/10.5194/acp-12-1031-2012

McComiskey, A., Feingold, G., Frisch, A. S., Turner, D. D., Miller, M. A., Chiu, J. C., et al. (2009). An assessment of aerosol-cloud interactions in marine stratus clouds based on surface remote sensing. *Journal of Geophysical Research*, *114*, D09203. https://doi.org/10.1029/2008JD011006

Menon, S., Del Genio, A. D., Kaufman, Y., Bennartz, R., Koch, D., Loeb, N., & Orlikowski, D. (2008). Analyzing signatures of aerosol-cloud interactions from satellite retrievals and the GISS GCM to constrain the aerosol indirect effect. *Journal of Geophysical Research*, *113*, D14S22. https://doi.org/10.1029/2007JD009442

Michibata, T., Suzuki, K., Sato, Y., & Takemura, T. (2016). The source of discrepancies in aerosol–cloud–precipitation interactions between GCM and A-train retrievals. *Atmospheric Chemistry and Physics*, *16*, 15,413–15,424. https://doi.org/10.5194/acp-16-15413-2016

Nakajima, T., Higurashi, A., Kawamoto, K., & Penner, J. E. (2001). A possible correlation between satellite derived cloud and aerosol microphysical parameters. *Geophysical Research Letters*, *28*(7), 1171–1174. https://doi.org/10.1029/2000GL012186

National Research Council (2005). *Radiative forcing of climate change: Expanding the concept and addressing uncertainties*. Washington, DC: The National Academies Press.

Neubauer, D., Christensen, M. W., Pooulsen, C. A., & Lohmann, U. (2017). Unveiling aerosol–cloud interactions. Part 2: Minimizing the effects of aerosol swelling and wet scavenging in ECHAM6-HAM2 for comparison to satellite data. *Atmospheric Chemistry and Physics*, *17*(21), 13,165–13,185. https://doi.org/10.5194/acp-17-13165-2017

Painemal, D., & Zuidema, P. (2013). The first aerosol indirect effect quantified through airborne remote sensing during VOCALS-rex. *Atmospheric Chemistry and Physics*, *13*(2), 917–931. https://doi.org/10.5194/acp-13-917-2013

Pandithurai, G., Dipu, S., Prabha, T. V., Maheskumar, R. S., Kulkarni, J. R., & Goswami, B. N. (2012). Aerosol effect on droplet spectral dispersion in warm continental cumuli. *Journal of Geophysical Research*, *117*, D16202. https://doi.org/10.1029/2011JD016532

Pandithurai, G., Takamura, T., Yamaguchi, J., Miyagi, K., Takano, T., Ishizaka, Y., et al. (2009). Aerosol effect on cloud droplet size as monitored from surface-based remote sensing over East China Sea region. *Geophysical Research Letters*, *36*, L13805. https://doi.org/10.1029/2009GL038451

Panicker, A. S., Pandithurai, G., & Dipu, S. (2010). Aerosol indirect effect during successive contrasting monsoon seasons over Indian subcontinent using MODIS data. *Atmospheric Environment*, *44*(15), 1937–1943. https://doi.org/10.1016/j.atmosenv.2010.02.015

Peng, J. F., Hu, M., Guo, S., Du, Z. F., Zheng, J., Shang, D. J., et al. (2016). Markedly enhanced absorption and direct radiative forcing of black carbon under polluted urban environments. *Proceedings of the National Academy of Sciences USA*, *113*, 4266–4271. https://doi.org/10.1073/pnas.1602310113

Quaas, J., & Boucher, O. (2005). Constraining the first aerosol indirect radiative forcing in the LMDZ GCM using POLDER and MODIS satellite data. *Geophysical Research Letters*, *32*, L17814. https://doi.org/10.1029/2005GL023850

Quaas, J., Boucher, Q., & Bréon, F. M. (2004). Aerosol indirect effects in POLDER satellite data and in the LMDZ GCM. *Journal of Geophysical Research*, *109*, D08205. https://doi.org/10.1029/2003JD004317

Quaas, J., Ming, Y., Menon, S., Takemura, T., Wang, M., Penner, J. E., et al. (2009). Aerosol indirect effects—General circulation model intercomparison and evaluation with satellite data. *Atmospheric Chemistry and Physics*, *9*(22), 8697–8717. https://doi.org/10.5194/acp-9-8697-2009

Quaas, J., Stevens, B., Stier, P., & Lohmann, U. (2010). Interpreting the cloud cover—Aerosol optical depth relationship found in satellite data using a general circulation model. *Atmospheric Chemistry and Physics*, *10*(13), 6129–6135. https://doi.org/10.5194/acp-10-6129-2010

Rosenfeld, D., & Feingold, G. (2003). Explanation of discrepancies among satellite observation of aerosol indirect effects. *Geophysical Research Letters*, *30*(14), 1776. https://doi.org/10.1029/2003GL017684

Rosenfeld, D., Zheng, Y., Hashimshoni, E., Pöhlker, M. L., Jefferson, A., Pöhlker, C., et al. (2016). Satellite retrieval of cloud condensation nuclei concentrations by using clouds as CCN chambers. *Proceedings of the National Academy of Science USA*, *113*, 5828–5834. https://doi.org/10.1073/pnas.1514044113

Seinfeld, J. H., Bretherton, C., Carslaw, K. S., Coe, H., DeMott, P. J., Dunlea, E. J., et al. (2016). Improving our fundamental understanding of the role of aerosol-cloud interactions in the climate system. *Proceedings of the National Academy of Science USA*, *113*, 5781–5790. https://doi.org/10.1073/pnas.1514043113

Stevens, B., & Feingold, G. (2009). Untangling aerosol effects on clouds and precipitation in a buffered system. *Nature*, *461*(7264), 607–613. https://doi.org/10.1038/nature08281

Su, W., Loeb, N. G., Xu, K. M., Schuster, G. L., & Eitzen, Z. A. (2010). An estimate of aerosol indirect effect from satellite measurements with concurrent meteorological analysis. *Journal of Geophysical Research*, *115*, D18219. https://doi.org/10.1029/2010JD013948

Tang, J., Wang, P., Mickley, L. J., Xia, X., Liao, H., Yue, X., & Xia, J. (2014). Positive relationship between liquid cloud droplet effective radius and aerosol optical depth over eastern China from satellite data. *Atmospheric Environment*, *84*, 244–253. https://doi.org/10.1016/j.atmosenv.2013.08.024

Tas, E., Koren, I., & Altaratz, O. (2012). On the sensitivity of droplet size relative dispersion to warm cumulus cloud evolution. *Geophysical Research Letters*, *39*, L13807. https://doi.org/10.1029/2012GL052157

Twomey, S. (1974). Pollution and the planetary albedo. *Atmospheric Environment*, *8*(12), 1251–1256. https://doi.org/10.1016/0004-6981(74)90004-3

Twomey, S. (1977). The influence of pollution on the shortwave albedo of clouds. *Journal of the Atmospheric Sciences*, *34*(7), 1149–1152. https://doi.org/10.1175/1520-0469(1977)034%3C1149:TIOPOT%3E2.0.CO;2

Wang, Y., Khalizov, A., Levy, M., & Zhang, R. (2013). Light absorbing aerosols and their atmospheric impacts. *Atmospheric Environment*, *81*, 713–715. https://doi.org/10.1016/j.atmosenv.2013.09.034

Wang, Z., & Sassen, K. (2001). Cloud type and macrophysical property retrieval using multiple remote sensors. *Journal of Applied Meteorology*, *40*(10), 1665–1682. https://doi.org/10.1175/1520-0450(2001)040%3C1665:CTAMPR%3E2.0.CO;2

Yang, W., Marshak, A., Várnai, T., & Wood, R. (2014). CALIPSO observations of near-cloud aerosol properties as a function of cloud fraction. *Geophysical Research Letters*, *41*, 9150–9157. https://doi.org/10.1002/2014GL061896

Yuan, T., Li, Z., Zhang, R., & Fan, J. (2008). Increase of cloud droplet size with aerosol optical depth: An observation and modeling study. *Journal of Geophysical Research*, *113*, D04201. https://doi.org/10.1029/2007JD008632